Original Article

A Deep Learning Approach Toward Differentiating Left versus Right for Idiopathic Ventricular Arrhythmia Originated from Outflow Tract

Reza Talebzadeh[1], Hossein Khosravi[1], Majid Haghjoo[2], Bahador Makki Abadi[3,4]

[1]Faculty of Electrical Engineering, Shahrood University of Technology, Shahrood, Iran, [2]Department of Cardiac Electrophysiology, Rajaie Cardiovascular Medical and Research Institute, Iran University of Medical Sciences, Tehran, Iran, [3]Department of Medical Physics and Biomedical Engineering, Tehran University of Medical Science, Tehran, Iran, [4]Research Center for Biomedical Technologies and Robotics, Advanced Medical Technologies and Equipment Institute, Tehran University of Medical Sciences, IKHC Hospital, Tehran, Iran

Abstract

Background: Idiopathic ventricular arrhythmia (VA) is among the common cardiac diseases, ranging from benign conditions to those requiring immediate medical intervention. Many VAs originate from the heart's outflow tract (OT). However, this area's complexity and small size, along with other influencing external factors, pose significant challenges to accurate diagnosis. The similarity of the features of VAs on the electrocardiogram (ECG) originating from the right or left side of the OT may lead to misdiagnosis. This study aims to detect the site of origin for VAs originating from the OT, which is important as a key precognition for treatment during catheter ablation. **Methods:** We perform this diagnosis using the standard 12-lead ECG and deep learning (DL) techniques without additional equipment. First, inspired by next-generation sequencing in genetics, we created one-dimensional (1D) streams of premature beats from a public dataset of 334 patients. Then, to compare the performance of common 1D DL models, the data were presented to various models, including long short-term memory, gated recurrent unit, and 1D convolutional neural network (1D-CNN). **Results:** Experimental results show that the 1D-CNN network achieves the best performance, with an accuracy of 93.4% and an F1-score of 0.9313. **Conclusions:** The findings demonstrate the effectiveness of DL in a higher level of applications, specifically in the treatment process, compared to conventional ECG analysis applications based on computerized methods. This represents a promising prospect for use in treatment processes without relying on complex and multifaceted diagnostic methods in the future.

Keywords: *Catheter ablation, electrocardiogram, heart disease, idiopathic ventricular arrhythmia, left ventricular outflow tract, outflow tract, right ventricular outflow tract*

Submitted: 06-Jan-2025 **Revised:** 24-Feb-2025 **Accepted:** 08-Apr-2025 **Published:** 01-Oct-2025

Introduction

With the continuous advancement of diagnostic technologies, research on identifying the region responsible for premature beats as a preablation strategy is increasing. Finding noninvasive methods with suitable diagnostic accuracy before performing radiofrequency ablation is significant, as it can increase the success rate of the procedure and reduce the duration of the treatment process and the risk of infection. Various approaches currently exist for performing this localization in patients with idiopathic ventricular arrhythmia (IVA). However, these approaches can be influenced by several factors, such as changes in lead positioning during electrocardiogram (ECG) acquisition,[1] variations in the torso from one individual to another, or limiting factors such as the need for additional equipment for diagnosis.[2]

In a practical and accessible approach, various algorithms based on 12-lead ECG have been proposed to determine the origin of ventricular activation in human studies. Most studies in this field have aimed for optimal accuracy by conducting manual analyses and identifying common patterns.[3-7] Yoshida *et al*. demonstrated the effective performance of the V2S/V3R index for differentiating between the left ventricular outflow tract (LVOT) and the right ventricular outflow tract (RVOT), independent of the site of the precordial transition.[8] He *et al*. developed a preablation diagnostic model by analyzing various methods on data from 488 patients (439 patients for RVOT and 49 patients for LVOT). This model

How to cite this article: Talebzadeh R, Khosravi H, Haghjoo M, Abadi BM. A deep learning approach toward differentiating left versus right for idiopathic ventricular arrhythmia originated from outflow tract. J Med Signals Sens 2025;15:28.

Address for correspondence:
Dr. Hossein Khosravi, Faculty of Electrical Engineering, Shahrood University of Technology, Daneshgah Blvd, Shahrood, Iran.
E-mail: hosseinkhosravi@shahroodut.ac.ir

Access this article online

Website: www.jmssjournal.net

DOI: 10.4103/jmss.jmss_2_25

Quick Response Code:

was based on two popular approaches, transition zone[9,10] and the V2S/V3R index, resulting in an LVOT detection sensitivity of 82% and specificity of 86%.[11]

Given the limitations of ECGs and the complexity of diagnosing certain regions such as outflow tract (OT), alternative methods such as torso imaging, noninvasive electrocardiographic imaging (ECGI), and view into ventricular onset have been recently developed.[12-16] However, the use of ECGI is relatively complex, requiring hundreds of leads from a single patient as well as skilled personnel for acquisition and interpretation.[17] Considering the complexity, time consumption, and need for additional equipment in these methods, ECG-based approaches continue to be widely applicable in electrophysiological studies because of their simplicity, accessibility, cost-effectiveness, and acceptable accuracy.

On the other hand, attention to deep learning (DL)-based technologies in medical applications is steadily increasing.[18-22] Reports indicate that using artificial intelligence algorithms can achieve higher accuracy in classifying and detecting the origins of premature ventricular contractions (PVCs) compared to human diagnostics.[23] There has also been an increasing focus on computer-based methods, particularly machine learning (ML) and recently DL in this field.[24-27]

Wang *et al*. proposed a two-stage classification method based on feature extraction and comparison among four ML algorithms.[28] The researchers used the second-stage algorithm to improve accuracy. The best accuracy reported was 76.84%. Chang *et al*. aimed to leverage DL to predict the origins of ventricular arrhythmias (VAs) involving the left ventricle (LV) and right ventricle (RV).[29] In their study, 3,628 PVCs were extracted from 731 patients, using a combination of two distinct datasets. A maximum of 20 PVCs per patient were manually extracted, with data processed over 1024 slices and fed into a six-layer CNN. The authors reported a sensitivity of 90.7% and a specificity of 92.3% for originated left-sided VAs. Similarly, Nakamura *et al*. performed a binary classification utilizing one-dimensional convolutional neural network (1D-CNN) to distinguish between RV and LV data. By extracting 464 PVCs from 111 patients, they achieved an accuracy of 87%.[23]

The OT is the common source of many IVAs.[30] The results suggest that the greatest difficulties in diagnosis occur within RVOT and LVOT regions, as the ECG features of RVOT-VAs and LVOT-VAs are similar, potentially leading to misdiagnosis.[7,31] Our study focuses on analyzing 12-lead ECG as one of the most accessible diagnostic tools, even in less developed areas, to differentiate the site of occurrence of IVAs arising from the OT. Due to the small size of the OT and the complex geometry of these regions and the position of RVOT and LVOT relative to standard ECG leads, site distinction in this area presents significant challenges. These challenges become even more pronounced when the origin is positioned in certain areas of this small region. The placement of RVOT and LVOT in the human heart is illustrated in Figure 1.

The research objective is pursued by PVC extraction and PVC stream generation inspired by next-generation sequencing (NGS). Subsequently, the performance of various 1D DL models will be evaluated to learn these streams for desired detection outcomes. Since the proposed method relies on detecting LVOT vs RVOT solely through the analysis of 12-lead ECGs by DL approaches, the results are expected to contribute to the integration and synchronization of signal acquisition with diagnostics. This approach aims to standardize initial diagnostic outcomes across different centers, even in less developed regions, and promote equitable access to treatment.

The remainder of the article is organized as follows: Section 2 introduces material and methods. Section 3 presents the experimental results of the implementation. Section 4 discusses the additional implementations conducted as the ablation study. Finally, Sections 5 and 6 cover the discussion and conclusions, respectively.

Materials and Methods

Learning algorithms

In this study, three widely used DL algorithms capable of learning 1D sequences were employed: long short-term memory (LSTM) networks, gated recurrent unit (GRU), and 1D-CNN. The LSTM network[32] is a type of Recurrent Neural Network (RNN) that can learn features over time series data. An LSTM layer learns long-term dependencies between time steps in sequence data. Compared to traditional RNNs, LSTMs can manage the retention or forgetting of information related to significant sections using control gates. Multiplicative gate units learn to regulate access to the constant error flow.[32] The advantage of LSTM networks over standard RNNs lies not only in the presence of control gates but also in their ability to prevent vanishing or exploding gradients. Furthermore, a bidirectional LSTM (BiLSTM) network was also utilized. In this network, learning occurs in both forward and backward directions. The BiLSTM network performs well with data such as ECG, where all samples are available from start to finish.[33]

GRU, such as LSTM, is another type of RNN. The primary difference between these two networks lies in how they control the memory cell state. In a GRU network, a gate controller manages the input and forget gates and two vectors from the LSTM cell are combined into a single vector. GRUs utilize less memory, which often results in faster performance compared to LSTMs. GRUs can be a suitable alternative to LSTMs, particularly when a simpler architecture is desired.

CNNs, inspired by human vision, were initially developed for predominantly two-dimensional applications. In recent years, a newer approach has emerged for utilizing the feature extraction capabilities of convolutional networks with 1D data, such as electrical signals. The introduction of 1D-CNNs has led to their increasing use in the analysis of 1D data.[34] CNNs leverage a hierarchical pattern in data analysis, gathering more complex patterns across various scales and enhancing filter bank approaches. These convolutional networks typically start with a convolutional layer, where the input signal passes through the convolutional layers to create feature maps or feature vectors. Subsequently, during the pooling stage, features are reduced, and stronger features are extracted from the feature maps. This process is repeated to an extent based on the input type to optimally derive the input motif with the strongest features. Finally, the resulting motif is presented as a feature vector to the fully connected layer, where the softmax function determines the final output of the network.

LSTM and GRU networks can retain information from previous time steps, whereas 1D-CNNs, despite their advantage of feature extraction through convolutional layers, require access to the raw input data in later layers due to their lack of memory.

Dataset

Training the network for this application requires specialized data. It is essential to allocate labels following successful catheter ablation (CA) and conducting patient follow-ups within similar and specific time frames. Due to the limitations in this field, merging multiple datasets is one of the approaches used. However, when combining different datasets, particularly multicenter data, it is crucial to ensure that data acquisition across all collections is carried out under the same standard conditions. For example, the correct placement of the leads during ECG acquisition can affect the results.[35] Even if all datasets used were collected specifically to identify the site of origin (SOO), it remains crucial to evaluate acquisition standards, conditions, environment, demographic characteristics of the cohort, uniformity of devices and processing methods, and signal digitization before generalizing results. In the absence of clear statements from dataset creators regarding these aspects, caution should be exercised when generalizing the results.

To the best of our knowledge, the only publicly available dataset for this application at the time of this research was recently published by Ningbo First Hospital of Zhejiang University.[36] As shown in Table 1, this dataset includes 334 ECG recordings captured during instances of PVC and ventricular tachycardia (VT). Of the total dataset, 77% of the recordings are attributed to RVOT, while 23% are associated with the LVOT. The signals are collected from 13 different origins within the OT. Approximately 18% of the data do not have defined regions within the OT.

Premature ventricular contraction selection and preprocessing

In this application, PVC extraction is important. Inputting signals into the network without PVC extraction can lead the network to focus on nontarget features. The Pan-Tompkins algorithm[36] and its generalized versions are among the most popular and widely utilized algorithms for fiducial points and QRS detection.[37-42] However, achieving generalizable automatic algorithms for accurately extracting ectopic beats remains a challenging issue due to the variability in the morphology of ectopic beats from different origins and under varying recording conditions. Given the significance of input data for distinguishing PVCs originating from RVOT vs LVOT, this extraction has frequently been performed manually in many studies.

In this research, we extracted the ectopic beats visually and similar to a clinical process. However, rather than extracting only the QRS complex and providing clean data to the network, the extraction of PVCs was conducted comprehensively and included other segments. In a clinical setting, validated PVCs are considered based on the characteristics desired by specialized physicians for electrophysiological studies. The initial diagnostic effort occurs during the electrophysiological study and before any ablation, relying on the electrophysiologist's experience and expertise.

For the analysis of candidate and confirmed PVCs, the extraction was performed randomly at an interval from one beat before to one beat after them without regard to fiducial or any other specific points. This extraction is such that PVC windows from the same origin in addition to different lengths and morphologies may or may not include a compensatory pause. Consequently, 946 complexes were verified under specialized supervision for final analysis. These complexes are not excessively clean, do not concentrate on a specific morphology of a PVC, and include additional characteristics beyond the QRS complex. PVC extraction from the ECG strip is shown in Figure 2.

To facilitate better comparisons, the noise reduction method proposed by the dataset developers was employed.[43] In addition, a normalization operation was uniformly applied to the sequences across each of the 12 leads within the range of − 1, +1. This process considered the maximum value, typically related to the highest R peak in all leads, and the minimum value per 12 leads. Thus, the determined maximum and minimum values may originate from different leads. This methodology preserves the proportional dimensions of the waves from each lead relative to the other leads for each PVC, including intervals and other fiducial characteristics. As previously stated, maintaining these ratios can be effectively useful for distinguishing RVOT vs LVOT.

In the proposed method, while maintaining the ratios during normalization and leveraging the features and

capabilities of DL, we do not initially focus on specific selected leads or measure selected morphologies in some leads compared to others. Instead, we allow the network to access all ratios in comparison to one another, enabling it to learn features across the entire PVC stream without performing manual feature extraction. Samples of PVCs originating from different and common sites are displayed simultaneously for all 12 leads in Figure 3. Visual similarities in the structure of PVCs from different sites and morphology differences for PVCs originating from common foci are observed in this figure. As illustrated in Figure 3, one of the complexities of diagnosis is the high morphological similarity of certain PVCs originating from OT. Furthermore, recognizing regions for which no specific origin has been recorded according to clinical standards in this dataset can complicate diagnosis, particularly if these regions are close to one another or exhibit significant similarity to foci on the opposite side. Finally, the windowed signals were uniformly downsampled from 2000 Hz to 500 Hz.

Preparing input data for the network

Although the disentangling of variations in the data is often regarded as a natural capability of deep neural networks, the extent of disentangling that can be achieved may be limited without specific design.[26] Accordingly, we employed a method for representing PVCs suitable for 1D networks. To this end, we created streams of extracted PVCs. The process of generating and analyzing PVC streams was inspired by NGS in genetics and the production of messenger RNA (mRNA) from DNA. The following describes how these streams are produced.

Next-generation sequencing

NGS provides a powerful tool in genetics for examining the exome or even the entire genome.[44] When genes are analyzed in a DNA sequence, each gene consists of exon and intron structures arranged together. Exons contain crucial information within these structures. Whole exome sequencing (WES)[45] is one of the latest methods in NGS.[46] All exons of a genome comprise an exome. In the WES approach, only the evaluation of exons, which hold significant information, is considered instead of the entire genome. WES allows for examining the coding regions of the genome to identify various genes related to specific disorders.[44] By arranging a sequence of exons, mRNA can be obtained, leading to the achievement of diagnostic targets through the resulting pattern matching. Therefore, rather than analyzing different parameters, the focus is intensified solely on the extracted exome. This process is illustrated in Figure 4.

Premature ventricular contraction streams generation

In the previous step, PVCs were extracted. This extraction approach, which does not precisely determine the start and end points based on the morphology of the PVCs and does not focus solely on the QRS, aims to minimize the detrimental effects on network diagnosis while preserving the beneficial impacts of the fiducial points. Introducing these factors into the network can expose the model to diverse states during learning, thereby reducing interpatient effects and the impact of distance-based decisions in complexes with well-defined start and end points on the diagnosis. This approach is useful for scenarios involving compensation pause with variable length, the presence or absence of the P wave, or structural changes due to PVC coupling. Consequently, this method avoids using clean and QRS-focused data, common in studies with similar objectives, or introducing nontarget features that could lead to artificially high diagnostic accuracy.

In this step, a sequence of PVCs from each of the 12 leads was generated in the order of aVF, aVL, aVR, I, II, III, and V1-V6. This sequence is regarded as the base or first segment of the final PVC stream. Next, repetition and concatenation of the PVC sequences were utilized to obtain the PVC stream. It is evident that, depending on the initial segments' lengths and the PVCs' morphology, the streams will have varying lengths. In addition to the QRS complex, all other waves and the compensation pause significantly influence the final structure of a PVC stream and may differ from one PVC to another. All PVC streams were cut

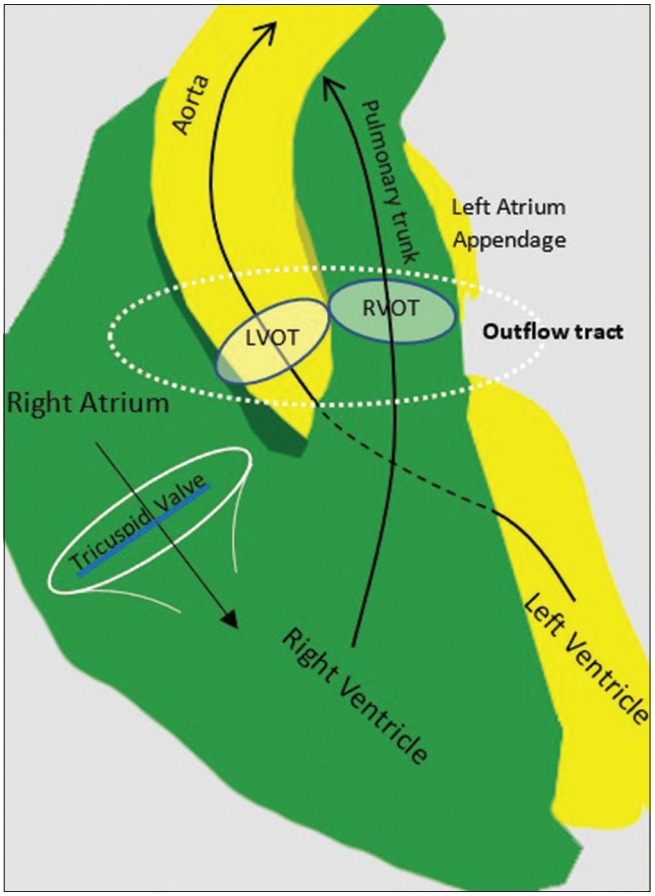

Figure 1: Schematic presentation of right ventricular outflow tract and left ventricular outflow tract positions in a lateral view of the right ventricle

in 25,000 samples. Based on the various lengths of primary streams, a minimum repetition for each PVC stream was two times. Ultimately, a downsampling was performed from 500 Hz to 30 Hz.

This drastic downsampling will help maintain the effects of important features such as QRS morphology, gradients, and other significant characteristics while minimizing the influence of details in peaks and troughs on recognition and network bias, allowing broader and more prominent indicators to have a larger impact on network learning. In addition, this downsampling will significantly enhance learning speed and detection performance by reducing the search space. Excessive downsampling can cause structural degradation and important information loss, especially in complexes. It is important to note that the second downsampling will be applied to each final PVC stream. Due to the inherent differences in PVCs and the method of creating PVC streams, this will lead to distinct variations in the structure of each stream, even among PVCs with the same focal point.

Thus, if we consider the cut regions from all 12 channels as significant genomes of these signals after extracting a PVC, we will create a stream that contains both exons and introns.

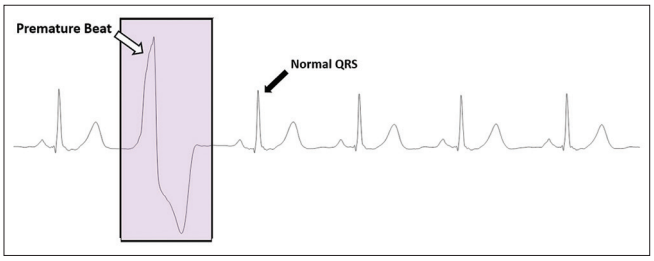

Figure 2: Premature ventricular contraction extraction from electrocardiogram

Due to the characteristics of ECG and PVC structure, performing a second downsampling step and drastically reducing the sample size removes some less essential information, and the data are effectively compressed while preserving the critical discriminating details. This second downsampling applied only to the PVC streams, may introduce intentional distortions, or eliminate some information, leading to greater differences among them. It is expected that through this method, strong distinguishing features and motifs for differentiating between RVOT and LVOT cases can be extracted by passing the data through network filters and performing pooling with an appropriate method. Subsequently, these streams, each containing 1563 samples after downsampling, will be fed into a 1D-CNN with the proposed architecture as the primary approach, alongside commonly used examples from other 1D deep networks as comparative methods, the features of which will be described in the next section. The proposed approach is illustrated in Figure 5.

Proposed model

In the 1D-CNN approach, a convolutional network with nine layers was utilized. Two 1D-CNN layers were responsible for extracting feature maps. Each convolutional layer employed a ReLU activation function, followed by layer normalization. The use of layer normalization not only accelerates the training process but also reduces the network's sensitivity to initialization. The specifications of the layers are presented in Table 2.

An important note for achieving effective learning in the proposed model using the 1D-CNN network is that the filter sizes must be sufficiently large. Given the structure of PVC streams, the filter sizes should be designed to allow simultaneous observation of several important features and

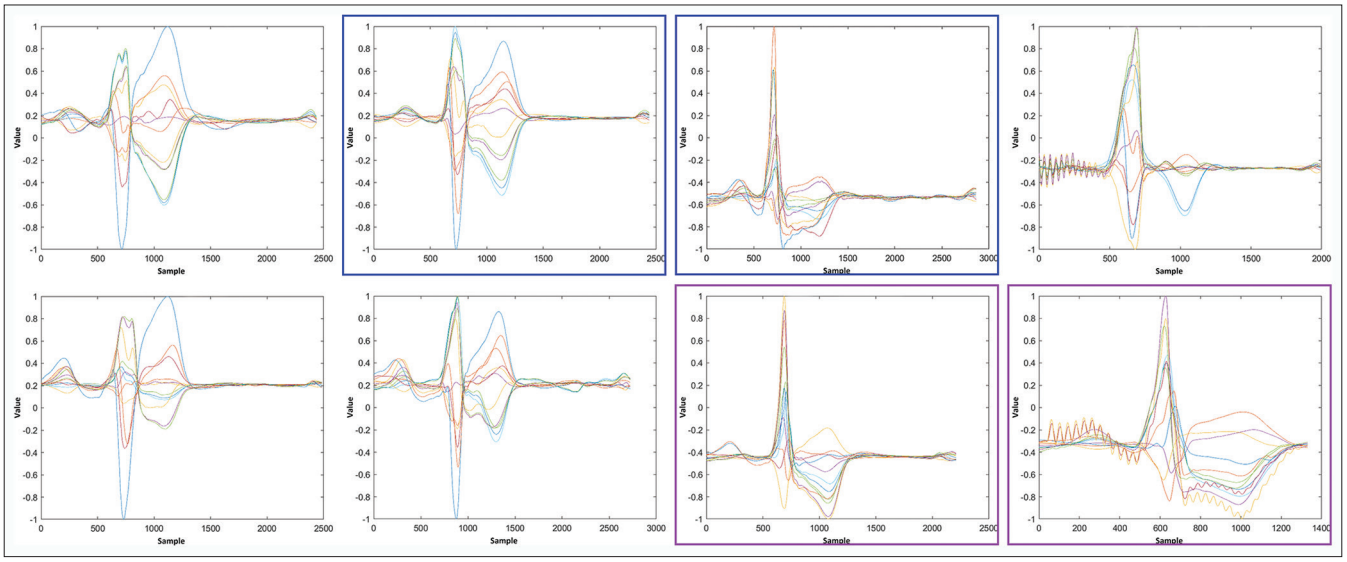

Figure 3: 12-lead display of premature ventricular contraction (PVC) samples originating from right ventricular outflow tract (top row) and left ventricular outflow tract (bottom row)

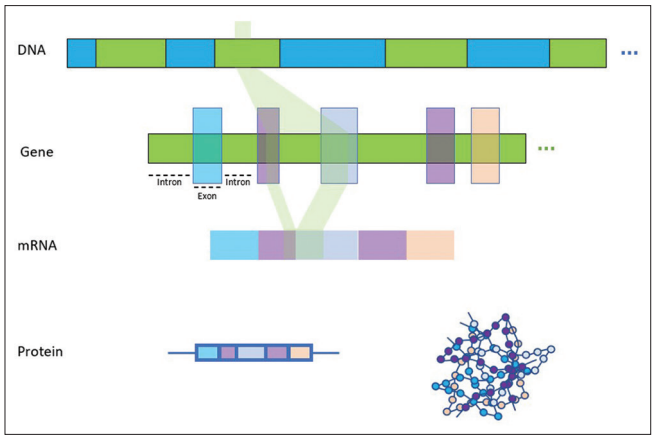

Figure 4: Exon graphical illustration from pre-messenger RNA to protein

the extraction of distinguishing characteristics. As the filters slide over the PVC stream, critical features throughout the sequence will be identified and stored in the corresponding feature maps, taking into account the variations present in different sections of each stream. Finally, by passing through a global max-pooling layer, only the most prominent distinguishing features are determined and arranged in a sequence, similar to a genetic code, and the final diagnosis can be achieved by matching their order placement. Based on the essence and structure of the input PVC streams, this code may vary for seemingly similar segments across different sections. This 1D sequence will correspond to the motifs related to the initial 12-channel PVCs. The graphical representation of the proposed model is shown in Figure 6.

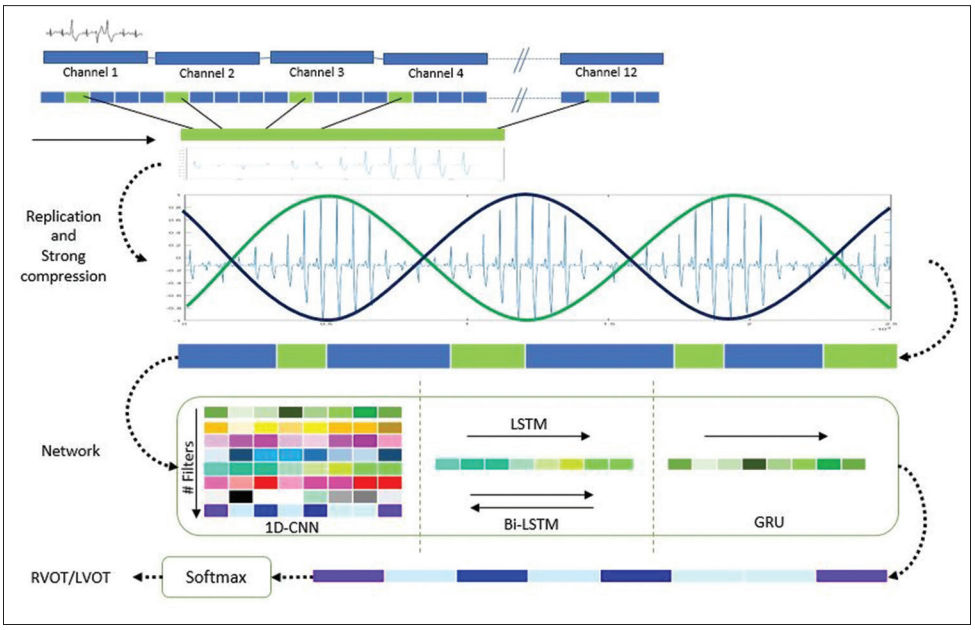

Figure 5: The proposed approach for localization of premature ventricular contractions

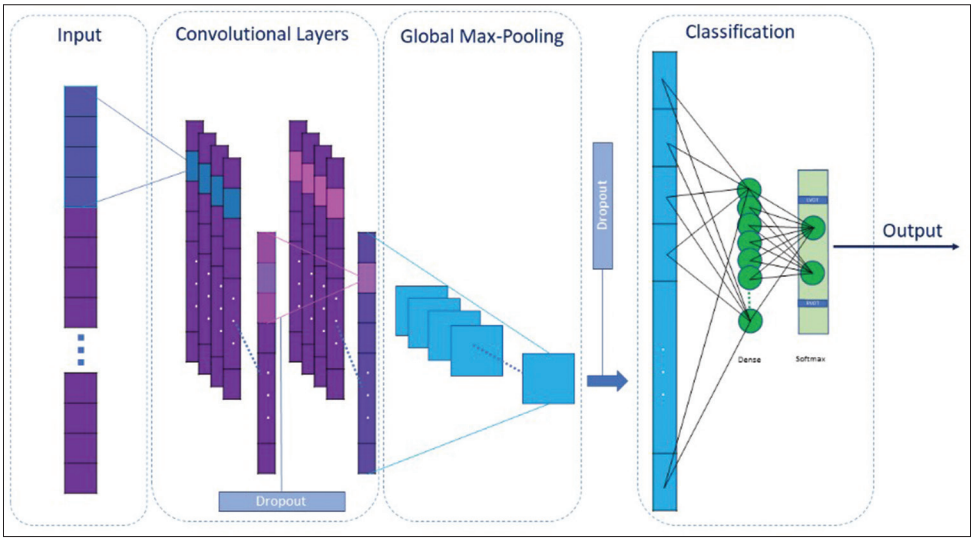

Figure 6: Proposed one-dimensional convolutional neural network model representation

Figure 7: Structures of the Recurrent Neural Network -based models

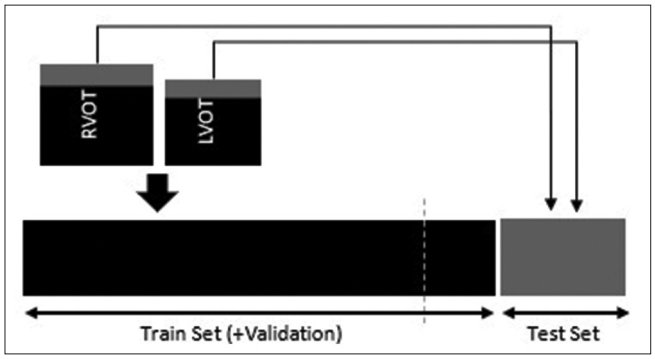

Figure 8: Training and test sets situation

In addition, we employed GRU, LSTM, and two widely used models based on LSTM cells: BiLSTM and Stacked-BiLSTM, to determine the most suitable network. To achieve the optimal number of convolutional layers and an appropriate number of filters, these parameters were gradually increased over several stages. The hidden units in the RNN-based models were set to 125 (BiLSTM-1, GRU-1) and 250 (BiLSTM-2, GRU-2). In the Stacked-BiLSTM model, the first layer used 250 hidden units, while the second layer utilized 125, structured according to prevalent designs in the relevant literature. We determined the optimal hyperparameters by experimenting with different configurations in a trial-and-error manner. The parameters in all networks were assessed with various adjustments across multiple stages and are reported based on the highest accuracies obtained. The structures are provided in Figure 7.

Evaluation metrics

The models were evaluated based on classification accuracy. A confusion matrix was used for performance and accuracy evaluation. Accordingly, four parameters were considered: true positives (TP), true negatives (TN), false positives (FP),

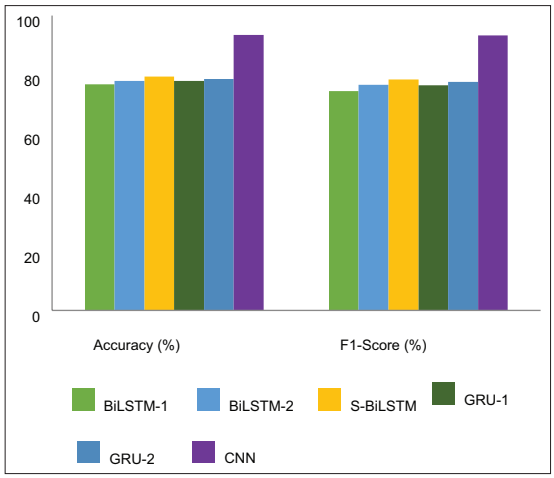

Figure 9: Comparison of the models for site of origin classification

and false negatives (FN). TP represents the number of LVOT observations correctly identified as LVOT, while TN indicates the correct identification of RVOT observations. FP refers to the number of RVOT observations incorrectly identified as LVOT, and FN denotes the number of LVOT observations incorrectly identified as RVOT. In addition to accuracy, model performance was evaluated using specificity, sensitivity, positive predictive value (PPV), and F1-score. These measures are defined based on TP, TN, FP, and FN, with their relationships summarized below:

$$Accuracy(\%) = \frac{TP+TN}{TP+TN+FP+FN} \times 100 \quad (1)$$

$$Specificity = \frac{TN}{TN+FP} \quad (2)$$

$$Sensitivity = \frac{TP}{TP+FN} \quad (3)$$

$$PPV = \frac{TP}{TP+FP} \quad (4)$$

$$F1-score = \frac{2TP}{TP+0.5(FP+FN)} \quad (5)$$

Experimental results

The implementation was conducted on a computer with Core i7@2.20GHz CPU, running 64-bit Windows 10 with 8GB of RAM, using Matlab 2022a. The dimensions of the dataset were 946 × 1563 × 1, as previously mentioned. Training data were balanced to ensure uniform data exposure and to prevent bias toward specific samples by the model. Hence, the number of samples on each side of OT was balanced to be 50% of the total set by oversampling. As shown in Figure 8, 80% of the data were selected for training and validation, and 20% were set aside for the test, ensuring no overlap between the datasets.

Initial weighting was performed using the Glorot method.[47] The Adam Optimizer was utilized for model training, as it has demonstrated good performance in

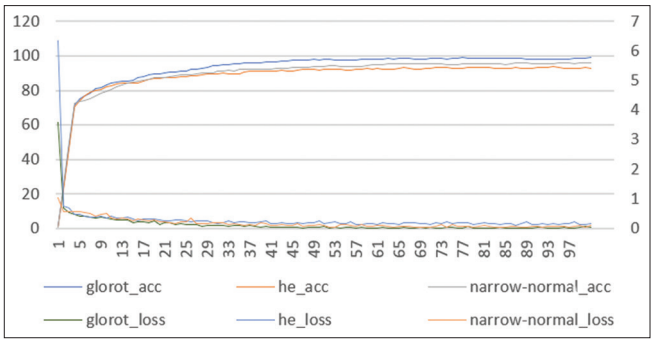

Figure 10: The smoothed learning curve of the proposed one-dimensional convolutional neural network model for three weight initialization methods

DL models. An L2 regularization value of 0.0001 was employed to prevent overfitting. Furthermore, a dropout rate of 50% was applied between learning layers and before the dense layer in all models. In addition to regularization and dropout, we implemented an early stopping strategy. Early stopping was applied based on the validation loss. If the validation loss increased, training was continued for five additional epochs. Training was terminated if the validation loss did not show improvement after these five epochs. The learning rate was set to 0.001, reduced by a factor of 0.7 every five epochs. The batch size is set to 64 and models are trained for 100 epochs. The vanilla LSTM network did not achieve satisfactory results. The implementation results for five other architectures, based on the best outcomes obtained, are shown in Table 3.

As indicated in Table 3, all RNN-based models almost achieved a near range of accuracy. However, in a single-layer structure with the same number of neurons, the GRU network achieved an accuracy of 78.47%, slightly better than the BiLSTM model with an accuracy of 77.74%. Although GRU can effectively continue learning to high epochs, learning may stop due to slower accuracy improvement compared to BiLSTM. Therefore, tuning the epochs and learning rate with an appropriate decay rate is crucial.

The Stacked-BiLSTM model reached an accuracy of 79.20% and an F1-score of 0.7833, demonstrating better detection compared to the single-layer BiLSTM and GRU models. The proposed model using 1D-CNN achieved an accuracy of 93.43%. In addition, the sensitivity, specificity, and F1-score were 0.8905, 0.9781, and 0.9313, respectively. Compared to other architectures, simultaneous high accuracy and PPV in this model indicate its suitability for the intended detection. A performance comparison of all models is shown in Figure 9.

The effect of using different layers with various kernel sizes in the proposed CNN model is shown in Table 4. This table shows performance, while the number of filters increases and the size of the filters decreases from one layer to the next. Accordingly, the best result was for the proposed model with two convolutional layers using kernel sizes of 99 for the first layer and 65 for the second layer.

According to this information, the best results were achieved for the proposed model with a PPV of 0.976 and an accuracy of 0.9313.

Ablation study

In this section, we examine performance by changing the proposed 1D-CNN model weight initialization. This contributes to a better understanding of the impact of different methods on accuracy. Furthermore, we assess the effect of the proposed data representation in the optimal structure.

Weight Initialization

The proposed model was trained using three weight initialization methods while keeping all hyperparameters constant. We evaluated three commonly used weight initializations: Glorot, He,[48] and Narrow-Normal. Figure 10 illustrates learning trends showing accuracy and learning error over 100 epochs for different initial weights. As shown in the figure, learning stops earlier with the He method than with the other two methods. However, an accuracy above 91.24% with Narrow-Normal at higher epochs seems achievable. The gradual increase in accuracy alongside a decreasing learning rate may lead to a training halt if the number of epochs is excessively high. The best result with a significant accuracy gap in fewer epochs was achieved when using the Glorot initialization.

Data presentation method

In this section, we evaluate the efficiency of the proposed method for presenting data to the network by comparing it with a basic approach. First, the PVC data from the 12 leads were arranged similarly to primary streams. All resulting 1D sequences were equalized in length by applying zero padding on the left side. Subsequently, all data were downsampled to 30 Hz, and training and test sets were presented to the proposed network. The accuracy of the basic approach was 89.78%. This finding suggests that extracting distinguishing features between RVOT and LVOT by repeatedly crossing from limb leads to chest leads and vice versa, as proposed, can be an effective approach for achieving better performance.

Discussion

Based on the results obtained in previous studies and considering the anatomical position of the OT within the heart and its location relative to the leads, RVOT exhibits the most overlap in diagnostic errors with LVOT. This is a significant challenge for differentiation, particularly in the cusps and this indistinguishable problem always requires further mapping in clinical practice to determine the activation origin.[23,27,29]

Table 5 compares the results of this study with other research focused on localizing the origin of activation within the OT using ECG. The number of studies that have independently and specifically addressed the differentiation of RVOT and LVOT using computational algorithms, particularly DL, remains limited. In most articles, PVCs arising from the OT are categorized collectively, or RVOT and LVOT differentiations are conducted alongside evaluations of the right and left ventricles. Given that the OT is the most common site for IVAs and considering its position and size relative to other ventricular regions, conducting focused studies on the differentiation between RVOT and LVOT could yield more accurate and reliable results. It is also important to note that employing algorithms for multi-class differentiation across all ventricular regions, while treating the OT as part of this categorization, could lead to artificially inflated accuracy rates and diminish the generalizability of the reported results.

Similar to many prevalent diagnoses by computerized algorithms in the cardiovascular field, one of the limitations and ongoing challenges in related research is the limited number of data and reporting results based on datasets with an uncertain or inappropriate distribution of data from different origins in OT. Having samples from various activation sites and origins within a single dataset or a combination of datasets is critical, especially for more complex sources, where adequate data samples are necessary for effective training and testing.

Most studies still rely on limited sample sizes.[49-52] Although the volume of analyzed data has increased in recent years, there is still a lack of public datasets with enough specialized data to compare the results of various methods across common datasets, especially for DL-based research. As shown in Table 5, several studies have addressed this limitation by combining different datasets or employing manual labeling through human annotation. It is important to note that these approaches can impact the model's learning process and limit the generalizability of its results.

Given the current limitations in accessing specialized data for this application, exploring various methods and approaches based on shared datasets can be pivotal in achieving optimal results. Public access to data can significantly enhance this process by clarifying the effectiveness of different methods and enabling robust comparisons of findings. In the present study, we utilized a publicly available dataset encompassing a suitable number and variety of PVC occurrences. As noted in Table 5, this approach may be more valuable than studies

Table 1: Statistical information of the dataset

	All	RVOT	LVOT
Patients, *n* (%)	334	257 (77)	77 (23)
Age (year), mean±SD	46.1±13.1	47.5±13.4	46.2±16.5
Male, *n* (%)	104 (31)	65 (25)	39 (50)

RVOT – Right ventricular outflow tract; LVOT – Left ventricular outflow tract; SD – Standard deviation

relying on simulated ECG signals or entirely personalized datasets or datasets with fewer data, thereby offering better opportunities for comparative analysis in future research.

The results of this study demonstrate the applicability and effectiveness of DL in identifying the SOO for PVCs. These findings are consistent with related studies.[25,26,29] However, ECG data analysis, whether performed using 12-lead recordings or 2D images,[29] tends to be more time-consuming compared to the 1D data approach utilized in this research. In addition, we applied a strong compression step to reduce the number of samples. Ultimately, a Global Max-Pooling layer was used to extract a condensed stream of the most significant indicators for PVC classification.

In ML-based methods,[23,24,27] manual feature extraction can be time-intensive, and focusing on fiducial points based on the morphology of PVCs often necessitates extensive trial and error. Nonetheless, ML algorithms can learn from fewer data based on the features extracted. However, in the research conducted by Zheng *et al*., there is a risk and possibility of adverse bias due to the small number of LVOT class samples compared to RVOT in the test.[53]

Avoiding manual feature extraction, along with reducing the computational load through analyzing 1D sequences with reduced samples and using widely used 1D deep network models, can provide two advantages of appropriate accuracy and speed together. In this study, DL models based on LSTM, GRU, and 1D-CNN, which have demonstrated proven effectiveness in learning time-series data, were analyzed in the intended application. According to the implementation results, the BiLSTM model performed better than LSTM, likely due to BiLSTM's ability to learn bidirectional dependencies. Although the GRU model demonstrated the fastest performance among RNN-based models due to its architectural features, the best results were obtained with the Stacked BiLSTM as model depth increased. The results indicated that the model's learning ability improved by adding BiLSTM layers.

This study identified the best performance using a 1D-CNN architecture with two convolutional layers. Further deepening of this model did not improve its accuracy. However, the proposed 1D-CNN model achieved the highest accuracy by a significant margin compared to the other models. While maintaining long-term temporal dependencies in the RNN-based models did not yield similar discriminative power. A comparison of Tables 3 and 4 shows that even with a single convolutional layer, the performance of 1D-CNN outperformed the Stacked BiLSTM and GRU models. This demonstrated the capability of 1D-CNN to extract distinguishing features from the generated streams, for the specific purpose of this research. This aligns with the findings by Bai *et al*., who noted that convolutional neural networks can perform comparably to or even better than RNNs in ordinary sequence modeling tasks. Moreover, a simple convolutional architecture can outperform conventional RNNs such as LSTMs across a diverse range of tasks and datasets.[54] The ability of 1D-CNN to extract complex patterns contributes to its superior performance over LSTM and GRU-based models when faced with more limited data. Furthermore, compared to these models, which learn long-term dependencies between time steps in sequence data, 1D-CNN can perform faster.

Given the significance of weight initialization and its impact on model learning, three commonly used initialization methods were compared to the proposed model. In the specific context of this study, the Glorot initialization method demonstrated superior performance in terms of both convergence speed and final accuracy. This result may be attributed to model architecture and the dataset used in this study. The relatively shallow depth of

Table 2: Specifications of the proposed 1D-convolutional neural network model layers and hyperparameters at optimal values

Layer	Type	Parameters
1	1D-CNN	96/99 (*n*/size) convolutions with stride 1 and ReLU activations
2	Layer normalization	-
3	Dropout	50%
4	1D-CNN	180/65 (*n*/size) convolutions with stride 1 and ReLU activations
5	Layer normalization	-
6	Max pooling	1-D global max pooling
7	Dropout	50%
8	Dense	2/Sigmoid
9	Output	Softmax

1D-CNN – 1D-convolutional neural network

Table 3: Implementation results

Type	Accuracy (%)	Specificity	Sensitivity	PPV	F1-score
BiLSTM-1	76.64	0.8540	0.6788	0.8230	0.7440
BiLSTM-2	77.74	0.8321	0.7226	0.8115	0.7645
GRU-1	77.74	0.8394	0.7153	0.8167	0.7626
GRU-2	78.47	0.8321	0.7372	0.8145	0.7739
Stacked BiLSTM	79.20	0.8321	0.7518	0.8175	0.7833
1D-CNN	93.43	0.9781	0.8905	0.9760	0.9313

BiLSTM-1 – Bidirectional long short-term memory-1; GRU: Gated recurrent unit; 1D-CNN – 1D-convolutional neural network; PPV – Positive predictive value

the model and the unique characteristics of the input data may have contributed to a more stable training process with the Glorot method. Furthermore, it is important to note that the effectiveness of weight initialization methods may vary depending on hyperparameter settings, model depth, and even the nature of the task.

However, this study does not delve further into exploring the underlying mechanisms through which different weight initialization methods influence model performance. Conducting such investigations would require extensive experimentation with variations in hyperparameters, layer configurations, and model architectures, including the evaluation of model depth and its interaction with different datasets, which is planned as future work. In addition, we aim to evaluate the performance of our approach for other diagnostic tasks, such as distinguishing PVCs from other arrhythmias, and its potential application in broader healthcare contexts.

Table 4: The proposed model implementation results using various kernel sizes

Model number	CNN (filters: *n*/size)			Accuracy (%)	F1-score
1	180/11	-	-	82.48	0.8235
2	180/33	-	-	84.78	0.8478
3	180/65	-	-	85.77	0.8550
4	180/99	-	-	87.32	0.8718
5	96/33	180/11	-	87.23	0.8797
6	96/65	180/33	-	92.70	0.9288
7	96/99	180/65	-	93.43	0.9313
8	96/99	180/65	300/33	90.51	0.9046

CNN – Convolutional neural network

Conclusion

Accurate diagnosis within the OT, which presents various complexities, is vital for mitigating risks during CA and advising patients. In this paper, we investigated the performance of three independent DL networks using 12-lead ECG data, leveraging several robust models to differentiate RVOT or LVOT. The performance of these models was evaluated by generating PVC streams without solely concentrating on QRS complex separation. This avoids learning clean data and the limitations and complexities of specifying and extracting waves' start and end points, such as the S wave, and focusing on specific parts of contractions. By reducing samples and presenting the data to the network in a 1D sequence, we decreased the computational burden. Optimal performance achieved with the proposed 1D-CNN model. Accordingly, the proposed approach can be used not only as an accessible

Table 5: Comparison of the proposed method with other related studies

References	Dataset	Annotation	Target	Number of patients	Method	Network (s)	Accuracy (%)
[24]	Private	Ablation	Multi-class (5)	87	ML	SVM	88.4
[25]	Private	Simulation	Multi-class (25/nonclinical)	-/(9)	DL	CNN	77.7
[26]	Private	Ablation	Left ventricular/multi-class (10)	39	DL	CNN	52.16–56.29
						SAE (LSTM-GRU)	
						f-SAE (LSTM-GRU)	
[27]	DB1: Private	Human annotation	Multi-class (11)	All: 249	ML	SVM	74
	DB2: INCARTDB			DB1: 211		RF	71.9
	DB3: EDGAR			DB2: 35		GBDT	72.5
				DB3: 3		GNB	71.2
[53]	Private+chapman-zhejiang	Ablation	RVOT versus LVOT	420	ML	ML	97
[23]	Private	Ablation	Right side versus left side of the heart	111	ML/DL	SVM	94
						CNN	87
[29]	Private+chapman-zhejiang	Ablation	RV versus LV	643	DL	CNN	92
				TPE: 356			
				CZJ: 287			
This study	Chapman-zhejiang	Ablation	RVOT versus LVOT	334	DL	GRU	78.47
						S-BiLSTM	79.20
						CNN	93.43

CNN – Convolutional neural network; RVOT – Right ventricular outflow tract; LVOT – Left ventricular outflow tract; RV – Right ventricle; LV – Left ventricle; BiLSTM – Bidirectional long short-term memory; GRU: Gated recurrent unit; DL – Deep learning; ML – Machine learning; LSTM – Long short-term memory; SVM - Support vector machine;TPE-Data from Taipei General Hospital; CZJ - Chapman-zhejiang dataset; RF - Random forest; GNB - Gaussian naïve bayes; GBDT: - Gradient-boosting decision tree; SAE: Sequential autoencoder; f-SAE - factor disentangling sequential autoencoder

method without additional equipment needed but also as a promising method in combination with other developing diagnostic methods as part of a multimodal analysis.

Financial support and sponsorship

Nil.

Conflicts of interest

There are no conflicts of interest.

References

1. Anter E, Frankel DS, Marchlinski FE, Dixit S. Effect of electrocardiographic lead placement on localization of outflow tract tachycardias. Heart Rhythm 2012;9:697-703.
2. Parreira L, Carmo P, Adragao P, Nunes S, Soares A, Marinheiro R, *et al.* Electrocardiographic imaging (ECGI): What is the minimal number of leads needed to obtain a good spatial resolution? J Electrocardiol 2020;62:86-93.
3. Betensky BP, Park RE, Marchlinski FE, Hutchinson MD, Garcia FC, Dixit S, *et al.* The V (2) transition ratio: A new electrocardiographic criterion for distinguishing left from right ventricular outflow tract tachycardia origin. J Am Coll Cardiol 2011;57:2255-62.
4. Kaypakli O, Koca H, Sahin DY, Karataş F, Ozbicer S, Koç M. S-R difference in V1-V2 is a novel criterion for differentiating the left from right ventricular outflow tract arrhythmias. Ann Noninvasive Electrocardiol 2018;23:e12516.
5. Zhao L, Li R, Zhang J, Xie R, Lu J, Liu J, *et al.* The R-S difference index: A new electrocardiographic method for differentiating idiopathic premature ventricular contractions originating from the left and right ventricular outflow tracts presenting a left bundle branch block pattern. Front. Physiol. 2022:13:1002926. doi: 10.3389/fphys.2022.1002926.
6. Zhang W, Huang K, Qu J, Su G, Li X, Kong Q, *et al*. A novel ECG algorithm to differentiate between ventricular arrhythmia from right versus left ventricular outflow tract. J Cardiovasc Med (Hagerstown) 2023;24:853-63.
7. Kepez A, Yildirim C, Gulsen K, Aslanger KE, Uslu A, Kup A, *et al.* Time to first nadir of the QRS complex in aVR/time to first nadir of the QRS complex in aVL: A novel method for distinguishing left from right outflow tract premature ventricular complexes (PVCs) with precordial transition in V3. J Electrocardiol 2025;88:153831.
8. Yoshida N, Yamada T, McElderry HT, Inden Y, Shimano M, Murohara T, *et al*. A novel electrocardiographic criterion for differentiating a left from right ventricular outflow tract tachycardia origin: The V2S/V3R index. J Cardiovasc Electrophysiol 2014;25:747-53.
9. Yoshida N, Inden Y, Uchikawa T, Kamiya H, Kitamura K, Shimano M, *et al.* Novel transitional zone index allows more accurate differentiation between idiopathic right ventricular outflow tract and aortic sinus cusp ventricular arrhythmias. Heart Rhythm 2011;8:349-56.
10. Yu M, Chen S, Zhang D, Shu Z, Tan X. To the editor – Correction of transitional zone index. Heart Rhythm 2011;8:e13-5.
11. He Z, Liu M, Yu M, Lu N, Li J, Xu T, *et al.* An electrocardiographic diagnostic model for differentiating left from right ventricular outflow tract tachycardia origin. J Cardiovasc Electrophysiol 2018;29:908-15.
12. Yu L, Jin Q, Zhou Z, Wu L, He B. Three-dimensional noninvasive imaging of ventricular arrhythmias in patients with premature ventricular contractions. IEEE Trans Biomed Eng 2018;65:1495-503.
13. Wang Y, Cuculich PS, Zhang J, Desouza KA, Vijayakumar R, Chen J, *et al.* Noninvasive electroanatomic mapping of human ventricular arrhythmias with electrocardiographic imaging. Sci Transl Med 2011;3:98ra84.
14. Healy L, Fitzpatrick N, Tahin T, Jauvert G, O'Brien J, Galvin J, *et al.* "31 Testing the validity of non-invasive PVC mapping technology VIVO™-view into ventricular onset with patients undergoing invasive PVC ablation-single centre experience." 2023;109:A35-A36.
15. Zhang J, Cooper DH, Desouza KA, Cuculich PS, Woodard PK, Smith TW, *et al.* Electrophysiologic scar substrate in relation to VT: Noninvasive high-resolution mapping and risk assessment with ECGI. Pacing Clin Electrophysiol 2016;39:781-91.
16. Kagan CM, Nguyen D, Ginnings TK, Amara R, Haq M, See V, *et al.* PO-666-06 first *in-vivo* evaluation of novel electrocardiography-imaging (ECG-I) system co-registered to clinical 3d mapping system to non-invasively predict vt and pvc ablation sites. Heart Rhythm, 2022;19:pp.S305-S306.
17. Pereira H, Niederer S, Rinaldi CA. Electrocardiographic imaging for cardiac arrhythmias and resynchronization therapy. Europace. 2020;22:1447-62. doi: 10.1093/europace/euaa165. Epub ahead of print. PMID: 32754737; PMCID: PMC7544539.
18. Zhao R, Xia Y, Wang Q. Dual-modal and multi-scale deep neural networks for sleep staging using EEG and ECG signals. Biomed Signal Process Control 2021;66:102455.
19. Yıldırım Ö, Baloglu UB, Acharya UR. A deep convolutional neural network model for automated identification of abnormal EEG signals. Neural Comput Appl 2020;32:15857-68.
20. RadhaMahendran S, Dogra A, Mendhe D, Babu SBT, Dixit S, Singh SP. Machine Learning for Drug Discovery: Predicting Drug-Protein Binding Affinities using Graph Convolutional Networks," 2024 5th International Conference on Recent Trends in Computer Science and Technology (ICRTCST), Jamshedpur, India, 2024, pp. 87-92, doi: 10.1109/ICRTCST61793.2024.10578506.
21. Jaiswal S, Gupta P. Diabetes prediction using Bi-directional long short-term memory. SN Comput Sci 2023;4:373.
22. Rizal S, Rahma YA. GRU-Based Fusion Models for Enhanced Blood Pressure Estimation From PPG Signals," in IEEE Access, 2024;12:pp. 80317-80326, doi: 10.1109/ACCESS.2024.3409741.
23. Nakamura T, Nagata Y, Nitta G, Okata S, Nagase M, Mitsui K, *et al.* Prediction of premature ventricular complex origins using artificial intelligence-enabled algorithms. Cardiovasc Digit Health J 2021;2:76-83.
24. Soheilykhah S, Sheikhani A, Sharif AG, Daevaeiha MM. Localization of premature ventricular contraction foci in normal individuals based on multichannel electrocardiogram signals processing. Springerplus 2013;2:486.
25. Yang T, Yu L, Jin Q, Wu L, He B. Localization of origins of premature ventricular contraction by means of convolutional neural network from 12-lead ECG. IEEE Trans Biomed Eng 2018;65:1662-71.
26. Gyawali PK, Horacek BM, Sapp JL, Wang L. Sequential factorized autoencoder for localizing the origin of ventricular activation from 12-lead electrocardiograms. IEEE Trans Biomed Eng 2020;67:1505-16.
27. He K, Nie Z, Zhong G, Yang C, Sun J. Localization of origins of premature ventricular contraction in the whole ventricle based on machine learning and automatic beat recognition from 12-lead ECG. Physiol Meas. 2020;41: 055007.
28. Wang Y, Feng X, Zhong G, Yang C. A "two-step classification" machine learning method for non-invasive localization of premature ventricular contraction origins based on 12-lead ECG. J Interv Card Electrophysiol 2024;67:457-70.

29. Chang TY, Chen KW, Liu CM, Chang SL, Lin YJ, Lo LW, *et al*. A high-precision deep learning algorithm to localize idiopathic ventricular arrhythmias. J Pers Med 2022;12:764.
30. Chen N, Wang L, Jiao J, Ju W, Wang Z, Zou C, *et al.* RV1+RV3 index to differentiate idiopathic ventricular arrhythmias arising from right ventricular outflow tract and aortic sinus of valsalva: A multicenter study. J Am Heart Assoc 2024;13:e033779.
31. Mariani MV, Piro A, Della Rocca DG, Forleo GB, Pothineni NV, Romero J, *et al.* Electrocardiographic criteria for differentiating left from right idiopathic outflow tract ventricular arrhythmias. Arrhythm Electrophysiol Rev 2021;10:10-6.
32. Hochreiter S, Schmidhuber J. Long short-term memory. Neural Comput 1997;9:1735-80.
33. Cho K, Van Merriënboer B, Gulcehre C, Bahdanau D, Bougares F, Schwenk H. Learning phrase representations using RNN encoder-decoder for statistical machine translation." arXiv preprint arXiv: 2014:1406.1078.
34. Kiranyaz S, Ince T, Gabbouj M. Real-time patient-specific ECG classification by 1-D convolutional neural networks. IEEE Trans Biomed Eng 2016;63:664-75.
35. Misra S, van Dam P, Chrispin J, Assis F, Keramati A, Kolandaivelu A, *et al.* Initial validation of a novel ECGI system for localization of premature ventricular contractions and ventricular tachycardia in structurally normal and abnormal hearts. J Electrocardiol 2018;51:801-8.
36. Pan J, Tompkins WJ. A real-time QRS detection algorithm. IEEE Trans Biomed Eng 1985;32:230-6.
37. Pinto JR, Cardoso JS, Lourenço A. Evolution, current challenges, and future possibilities in ECG biometrics. IEEE Access 2018;6:34746-76.
38. Sathyapriya L, Murali L, Manigandan T. Analysis and Detection R-Peak Detection Using Modified Pan-Tompkins Algorithm. In 2014 IEEE International Conference on Advanced Communications, Control and Computing Technologies. IEEE; 2014.
39. Shen TW, Tompkins WJ, Hu YH. Implementation of a one-lead ECG human identification system on a normal population. J Eng Comput Innov 2011;2:12-21.
40. Rahman MO, Augustyniak P, Olejarczyk E. The QRS Detection Using the Modified Pan-Tompkins Algorithm. In 2024 IEEE International Workshop on Metrology for Industry 4.0 and IoT (MetroInd4. 0 and IoT). IEEE; 2024.
41. Louis W, Komeili M, Hatzinakos D. Continuous Authentication Using one-Dimensional Multi-Resolution Local Binary Patterns (1DMRLBP) in ECG Biometrics. IEEE Transactions on Information Forensics and Security; 2016;11:2818-32.
42. Wu X, Wang Z, Xu B, Ma X. "Optimized pan-tompkins based heartbeat detection algorithms." In 2020 Chinese Control And Decision Conference (CCDC), 2020:pp. 892-897.
43. Zheng J, Fu G, Anderson K, Chu H, Rakovski C. A 12-Lead ECG database to identify origins of idiopathic ventricular arrhythmia containing 334 patients. Sci Data 2020;7:98.
44. Monroe GR, Frederix GW, Savelberg SM, de Vries TI, Duran KJ, van der Smagt JJ, *et al.* Effectiveness of whole-exome sequencing and costs of the traditional diagnostic trajectory in children with intellectual disability. Genet Med 2016;18:949-56.
45. Ewans LJ, Schofield D, Shrestha R, Zhu Y, Gayevskiy V, Ying K, *et al.* Whole-exome sequencing reanalysis at 12 months boosts diagnosis and is cost-effective when applied early in Mendelian disorders. Genet Med 2018;20:1564-74.
46. Schwarze K, Buchanan J, Taylor JC, Wordsworth S. Are whole-exome and whole-genome sequencing approaches cost-effective? A systematic review of the literature. Genet Med 2018;20:1122-30.
47. Glorot X, Bengio Y. Understanding the difficulty of training deep feedforward neural networks. In Proceedings of the Thirteenth International Conference on Artificial Intelligence and Statistics. JMLR Workshop and Conference Proceedings; 2010.
48. He K, Zhang X, Ren S, Sun J; Proceedings of the IEEE International Conference on Computer Vision (ICCV), 2015, pp. 1026-1034.
49. Zhou S, AbdelWahab A, Sapp JL, Sung E, Aronis KN, Warren JW, *et al*. Assessment of an ECG-based system for localizing ventricular arrhythmias in patients with structural heart disease. J Am Heart Assoc 2021;10:e022217.
50. Zhou S, AbdelWahab A, Horáček BM, MacInnis PJ, Warren JW, Davis JS, *et al*. Prospective assessment of an automated intraprocedural 12-lead ECG-based system for localization of early left ventricular activation. Circ Arrhythm Electrophysiol 2020;13:e008262.
51. Waight MC, Li AC, Leung LW, Wiles BM, Thomas GR, Gallagher MM, *et al*. Hourly variability in outflow tract ectopy as a predictor of its site of origin. J Cardiovasc Electrophysiol 2022;33:7-16.
52. Zhu X, Chen S, Ma K, Chen Z, Chen C, Jiang Z. Interventricular septum angle obtained from cardiac computed tomography for origin differentiation of outflow tract ventricular arrhythmia between left and right. Pacing Clin Electrophysiol 2022;45:1279-87.
53. Zheng J, Fu G, Abudayyeh I, Yacoub M, Chang A, Feaster WW, *et al*. A high-precision machine learning algorithm to classify left and right outflow tract ventricular tachycardia. Front Physiol 2021;12:641066.
54. Bai S, Kolter JZ, Koltun V. An empirical evaluation of generic convolutional and recurrent networks for sequence modeling. arXiv preprint arXiv: 2018:1803.01271.